

# Radiation effects on candidate fiber optic sensors for nuclear applications

Chris Petrie

Oak Ridge National Laboratory

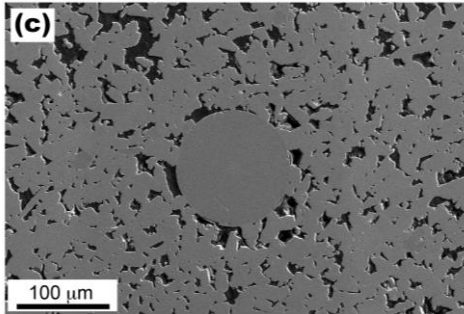
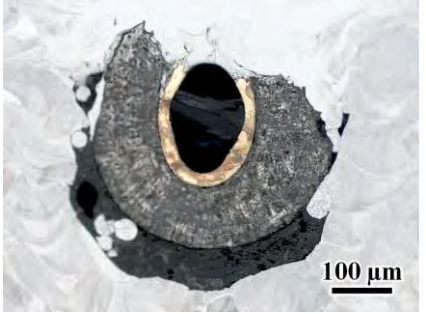
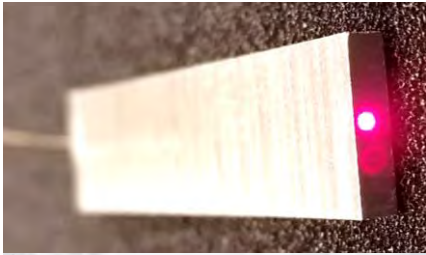
3/2/2023

ORNL is managed by UT-Battelle LLC for the US Department of Energy

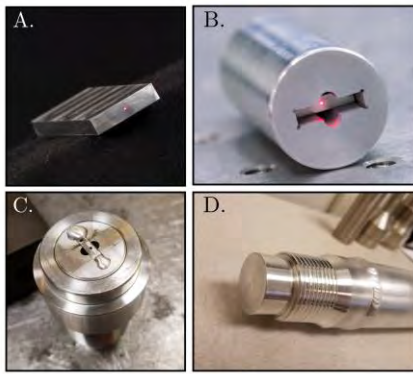
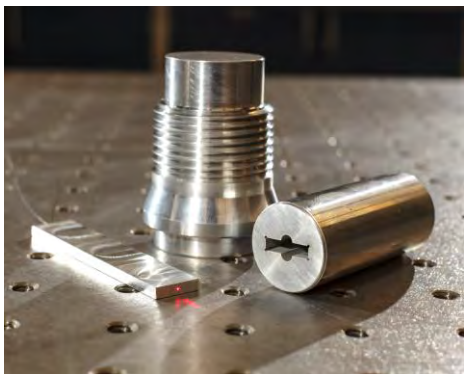
Contributions from:

Dan Sweeney, Holden Hyer, Brandon Wilson, Tony Birri,  
Tom Blue

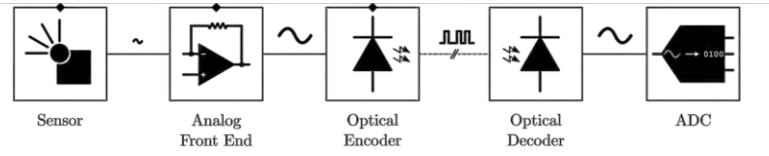
# Nuclear applications for fiber optics (not a comprehensive list)



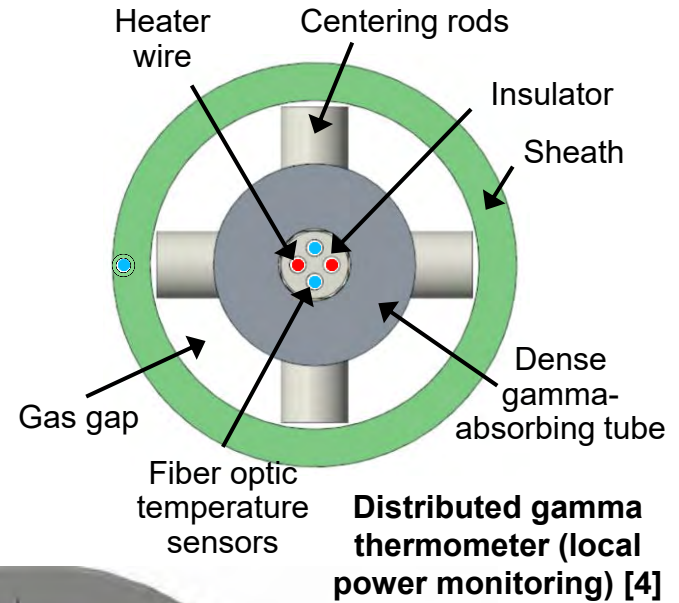
Fiber optic sensors embedded in 3D printed stainless steel (left) or SiC (right) for local strain or vibration monitoring [1, 2]



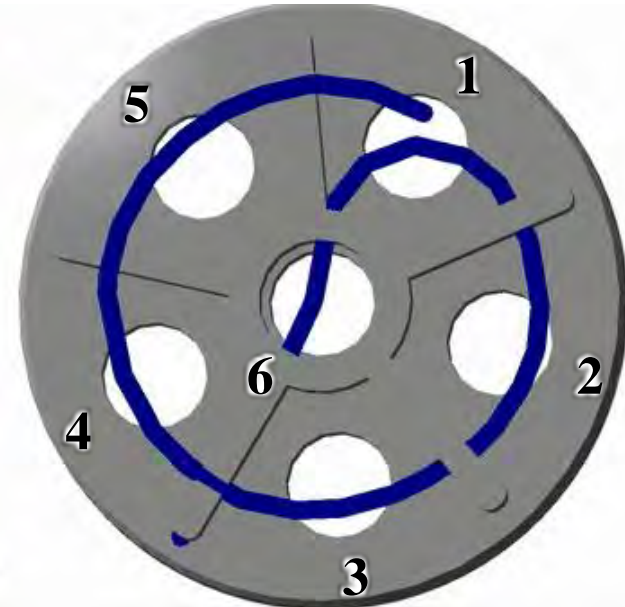
Embedded fiber optic sensor for measuring pressure, corrosion, or acoustic emissions [5, 6]



Rad-hard Front End Digitizer (FREND) to transmit conventional sensor data through reactor containment over fiber optic cables to reduce noise in cabling [3]



Distributed gamma thermometer (local power monitoring) [4]



Local temperature measurements in an experiment simulating gas-cooled reactor core outlet mixing [7]

[1] H.C. Hyer et al., *Additive Manufacturing*, **52** (2022), 102681.  
 [2] C.M. Petrie et al., *Journal of Nuclear Materials* **552** (2021) 153012.  
 [3] D.C. Sweeney et al., "Analog Front End Digitizer using Optical Pulse-Width Modulation for Nuclear Applications," *IEEE Trans. Instrum. Meas.* (under review)  
 [4] A. Birri and T.E. Blue, *Progress in Nuclear Energy* **130** (2020) 103552.

[5] D.C. Sweeney, A.M. Schrell, and C.M. Petrie, *IEEE Trans. Instrum. Meas.* **70** (2021) 1-10.  
 [6] C.M. Petrie, D.C. Sweeney, and Y. Liu, US Non-Provisional Patent No. US 2021/0033479 A1, Application No. 16/865,475, published February 4, 2021.  
 [7] H.C. Heyer et al., "Toward Local Core Outlet Temperature Monitoring in Gas-Cooled Nuclear Reactors Using Distributed Fiber-Optic Temperature Sensors," *Applied Thermal Engineering* (under review).

# Fiber optic sensor materials

## Fused silica glass ( $\alpha$ -SiO<sub>2</sub>)

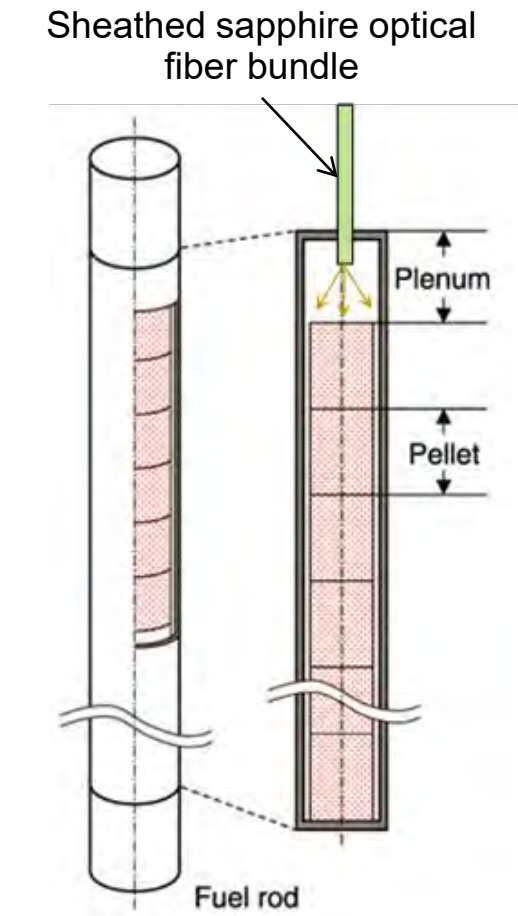
- Maximum temperature: 1000°C (long-term devitrification)
- Cost: As low as ~\$0.20 per meter
- Core diameter: ~8–10 μm (singlemode)
- Cladding: Routinely accomplished via chemical dopants in  $\alpha$ -SiO<sub>2</sub>
- Maximum continuous length: >> kilometers
- Typical intrinsic attenuation: ~dB/km

## Singe-crystal sapphire ( $\alpha$ -Al<sub>2</sub>O<sub>3</sub>)

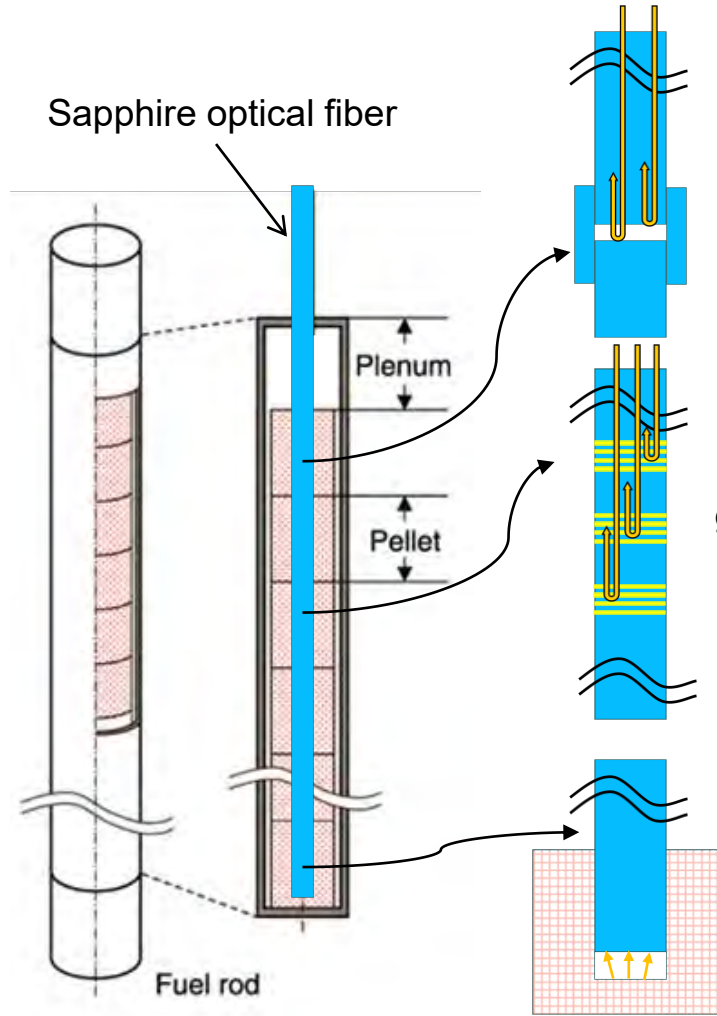
- Maximum temperature : 1700–1800°C demonstrated, close to ~2000°C melting point
- Cost: ~\$1k per meter
- Diameter: 75–500 μm
- Cladding: None
  - Active R&D targeting singlemode operation
- Maximum continuous length: ~meters
- Typical intrinsic attenuation: ~dB/m
  - Dominated by scattering losses due to lack of cladding
- Must be single-crystalline to avoid scattering losses at grain boundaries
- High loss and short lengths generally require non-trivial splicing to  $\alpha$ -SiO<sub>2</sub> leads



# Nuclear applications for sapphire fiber



**NIR borescope -  
Visualize fuel  
dimensional changes,  
cracking, relocation**

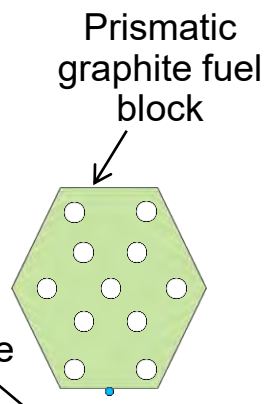


**Single-point or distributed  
measurement of fuel centerline  
temperature**

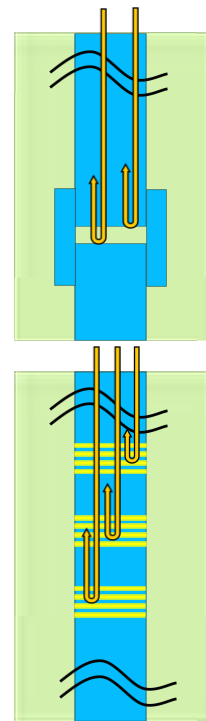
**Option 1:** Fabry-Perot cavity formed by  $\text{Al}_2\text{O}_3$  capillary tube (single point)

**Option 2:** Bragg gratings in sapphire fiber (distributed measurement)

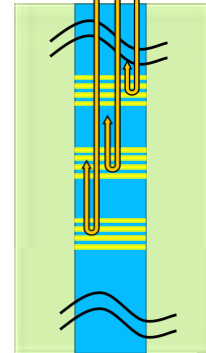
**Option 3:** Pyrometer (single point)



**Single-point or distributed measurement of strain or vibration in fuel or structural materials**



**Option 1:** Fabry-Perot cavity formed by  $\text{Al}_2\text{O}_3$  capillary tube (single point)

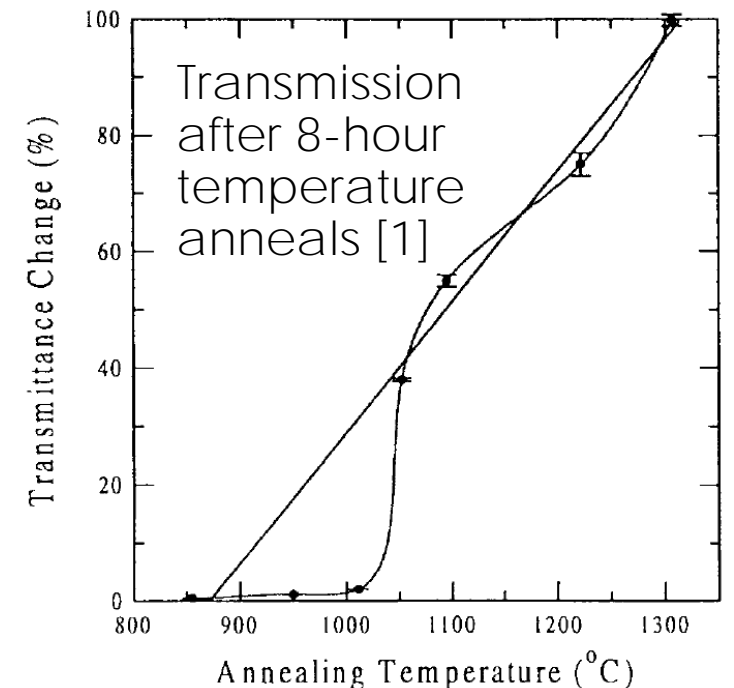
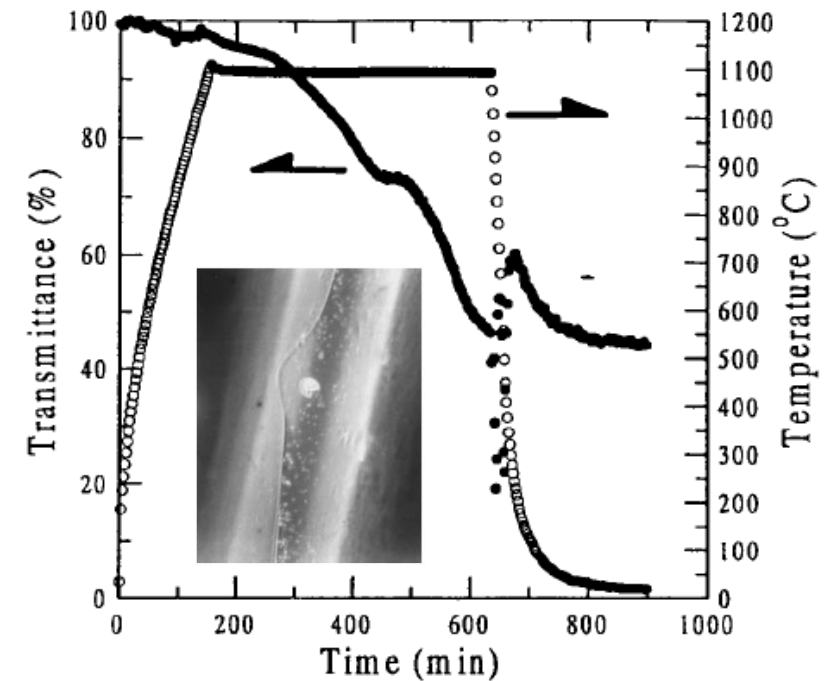


**Option 2:** Bragg gratings in sapphire fiber (distributed measurement)

# a-SiO<sub>2</sub>: High temperature degradation

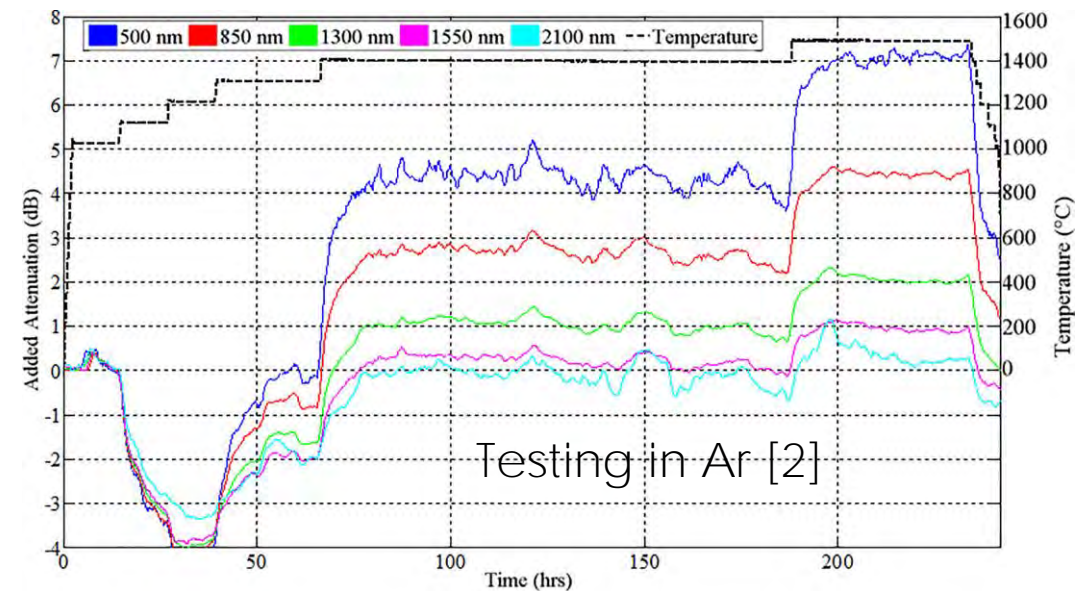
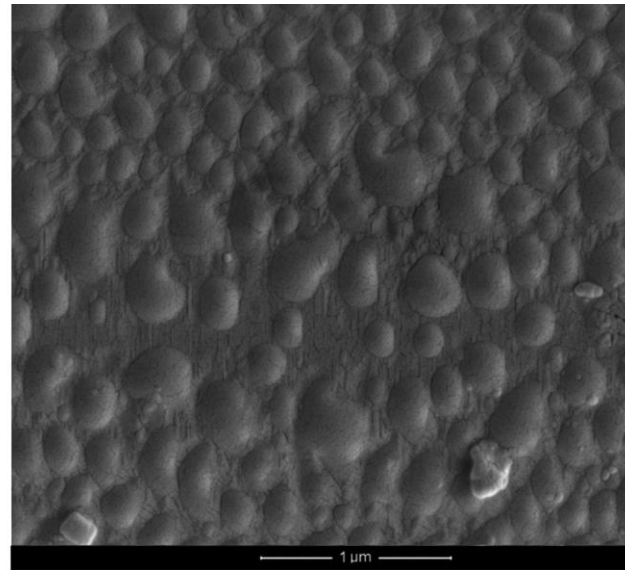
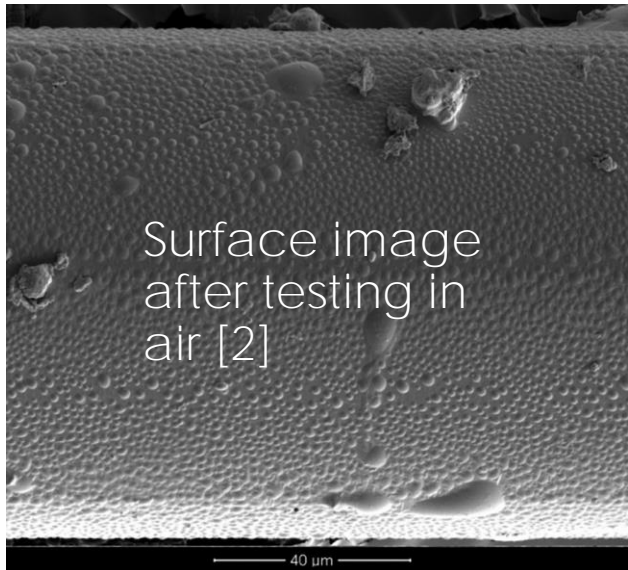
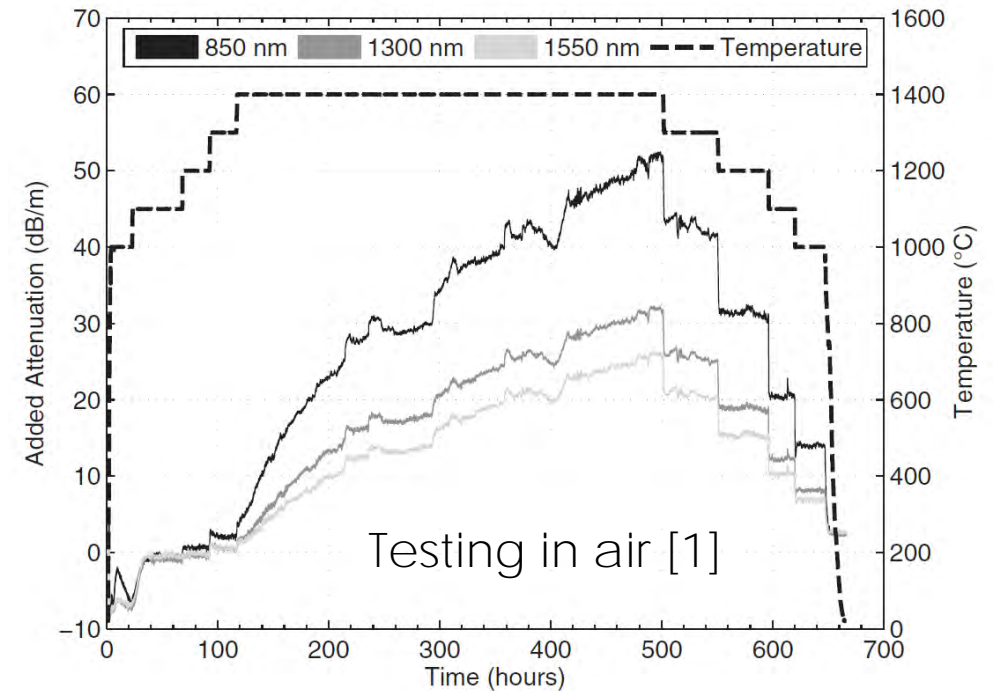
- Polymer-based coatings burn at ~200–300°C (requires metal coatings or sheaths for protection)
- Increased OH absorption near 1400 nm and > 1800 nm in presence of H<sub>2</sub> or H<sub>2</sub>O at > ~600°C (manageable)
- Increased O mobility at > 600°C
  - No significant effect on transmission
  - Can alter local defect distributions and challenge distributed temperature sensors relying on Rayleigh backscatter
  - Can be addressed by altering fiber or signal processing
- Dopant diffusion at > 1000°C
- Devitrification, or crystallization, at temperatures of ~900°C and above (rate depends on temperature)
  - 850°C: Indefinite?
  - 900°C: Days to weeks?
  - 1000°C: Days
  - 1100°C: <1 day

[1] A.H. Rose, "Devitrification in Annealed Optical Fiber," *Journal of Lightwave Technology* 15(1997) 808–814.



# $\alpha\text{-Al}_2\text{O}_3$ : High-temperature degradation

- Large increases in attenuation in air at  $\sim 1400^\circ\text{C}$ 
  - Formation of surface bubbles, likely aluminum hydroxide  $\text{Al}(\text{OH})_3$
- Attenuation and bubbles not observed in an inert environment
  - Promising for nuclear applications that can locate sapphire sensors in a metal sheath or fuel cladding backfilled with an inert gas
  - Successful operation up to  $1500^\circ\text{C}$



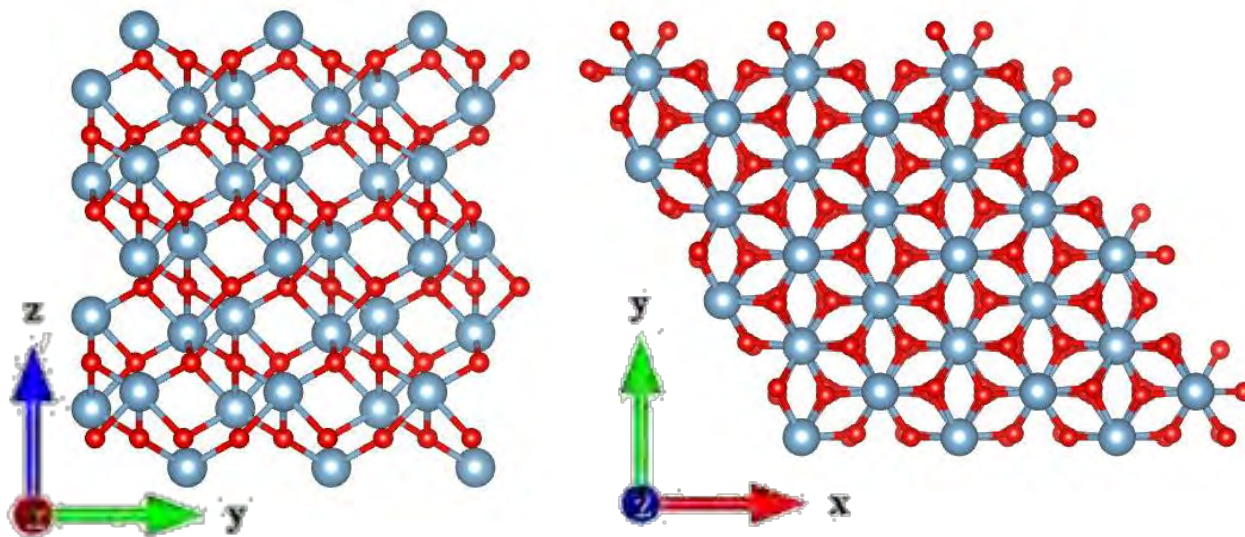
[1] C.M. Petrie and T.E. Blue, "In-situ Thermally Induced Attenuation in Sapphire Optical Fibers Heated to  $1400^\circ\text{C}$ ," *Journal of the American Ceramic Society* 98 (2014) 483-489.  
[2] B.A. Wilson et al., "High Temperature Effects on the Light Transmission through Sapphire Optical Fiber," *Journal of the American Ceramic Society* 101 (2018) 3452-3459.



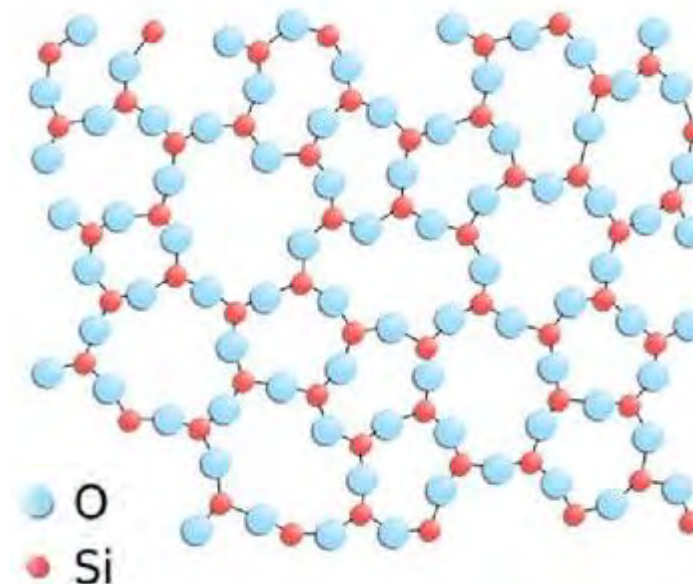
# Single crystal sapphire ( $\alpha\text{-Al}_2\text{O}_3$ ) vs. amorphous silicon dioxide ( $\text{a-SiO}_2$ )

- Sapphire: Ordered single crystalline structure (corundum)
  - Hexagonal close packing of O (anion sublattice), Al occupies 2/3 of octahedral interstices
  - No grain boundaries to serve as sinks for point defects
  - Point defects  $\rightarrow$  trapping states in band gap  $\rightarrow$  increased optical absorption at energies corresponding to band transitions
  - Aggregation of point defects can result in microstructural and dimensional changes that cause drift of Bragg gratings or other sensors that rely on changes in refractive index or thermal expansion
- Silica: Amorphous structure (distribution of Si-O-Si bond angles, no long-range order)
  - Less sensitive to point defects
  - Expected to be more tolerant to radiation damage

## Ordered crystal structure of $\alpha\text{-Al}_2\text{O}_3$



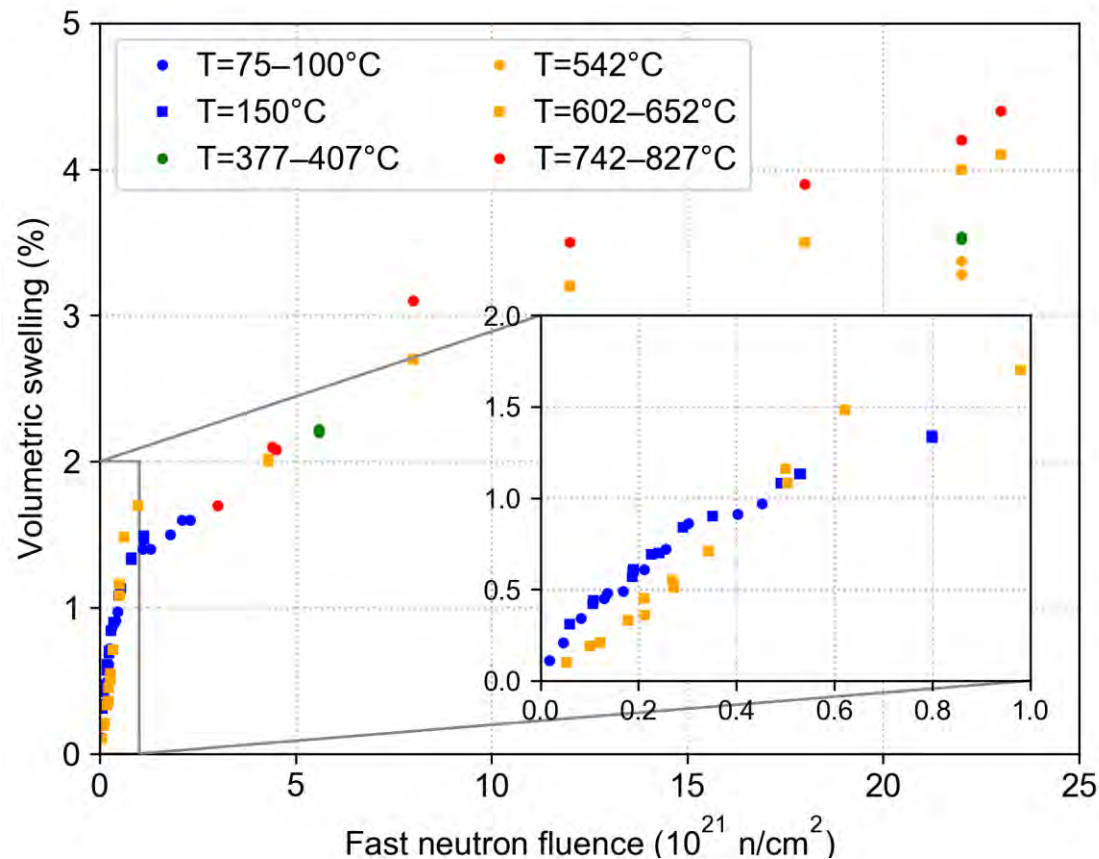
## Amorphous structure of $\text{a-SiO}_2$



# Radiation-induced dimensional changes

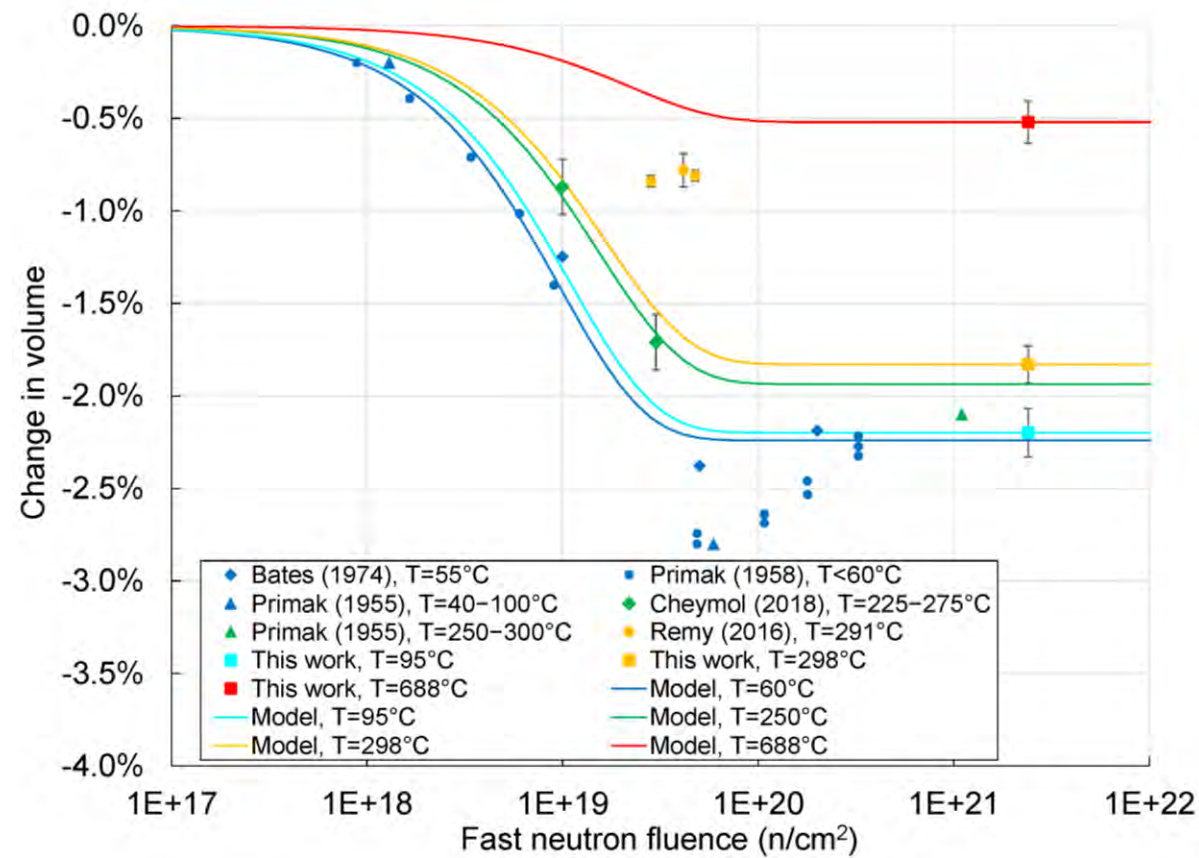
## Sapphire swells >4% under neutron irradiation [1]

- No evidence of saturation up to  $\sim 2.3 \times 10^{22}$  n/cm<sup>2</sup>
- Swelling higher at higher temperatures



## Fused silica compacts ~2% under neutron irradiation [2]

- Saturates after  $\sim 10^{20}$  n/cm<sup>2</sup>
- Equilibrium compaction lower at higher temperatures

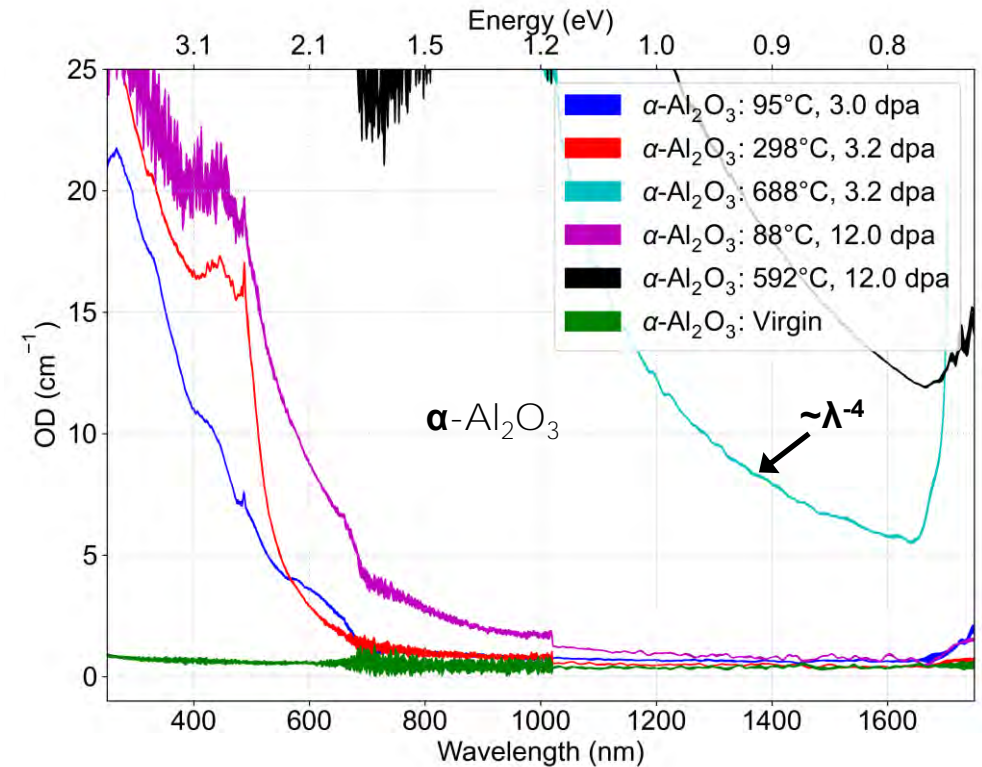
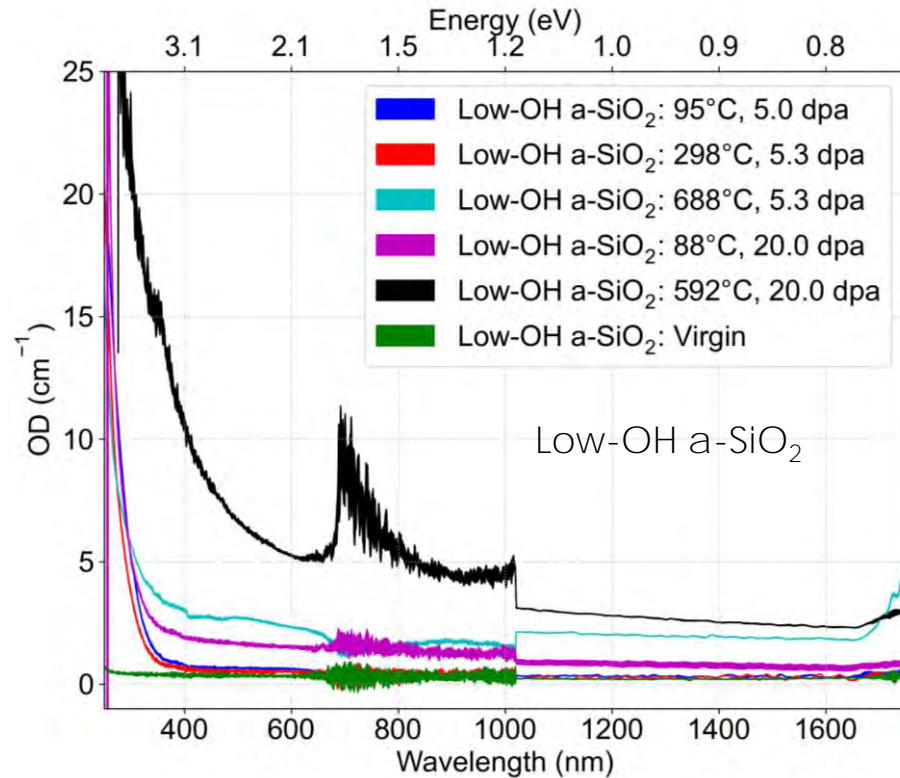
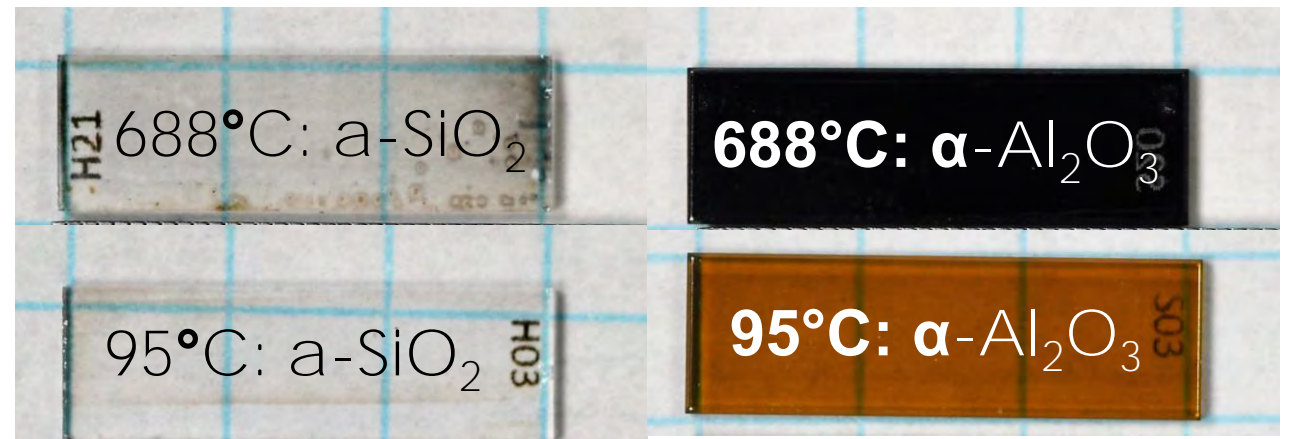


[1] C.M. Petrie et al., "Optical transmission and dimensional stability of single-crystal sapphire after high-dose neutron irradiation at various temperatures up to 688°C," *Journal of Nuclear Materials* 559 (2022) 153432.

[2] C.M. Petrie et al., "High-Dose Temperature-Dependent Neutron Irradiation Effects on the Optical Transmission and Dimensional Stability of Amorphous Fused Silica," *Journal of Non-Crystalline Solids* 525 (2019) 119668.



# High neutron fluence ( $\sim 10^{22}$ $n_{\text{fast}}/\text{cm}^2 = 12\text{--}20$ dpa) measurements of bulk optical properties

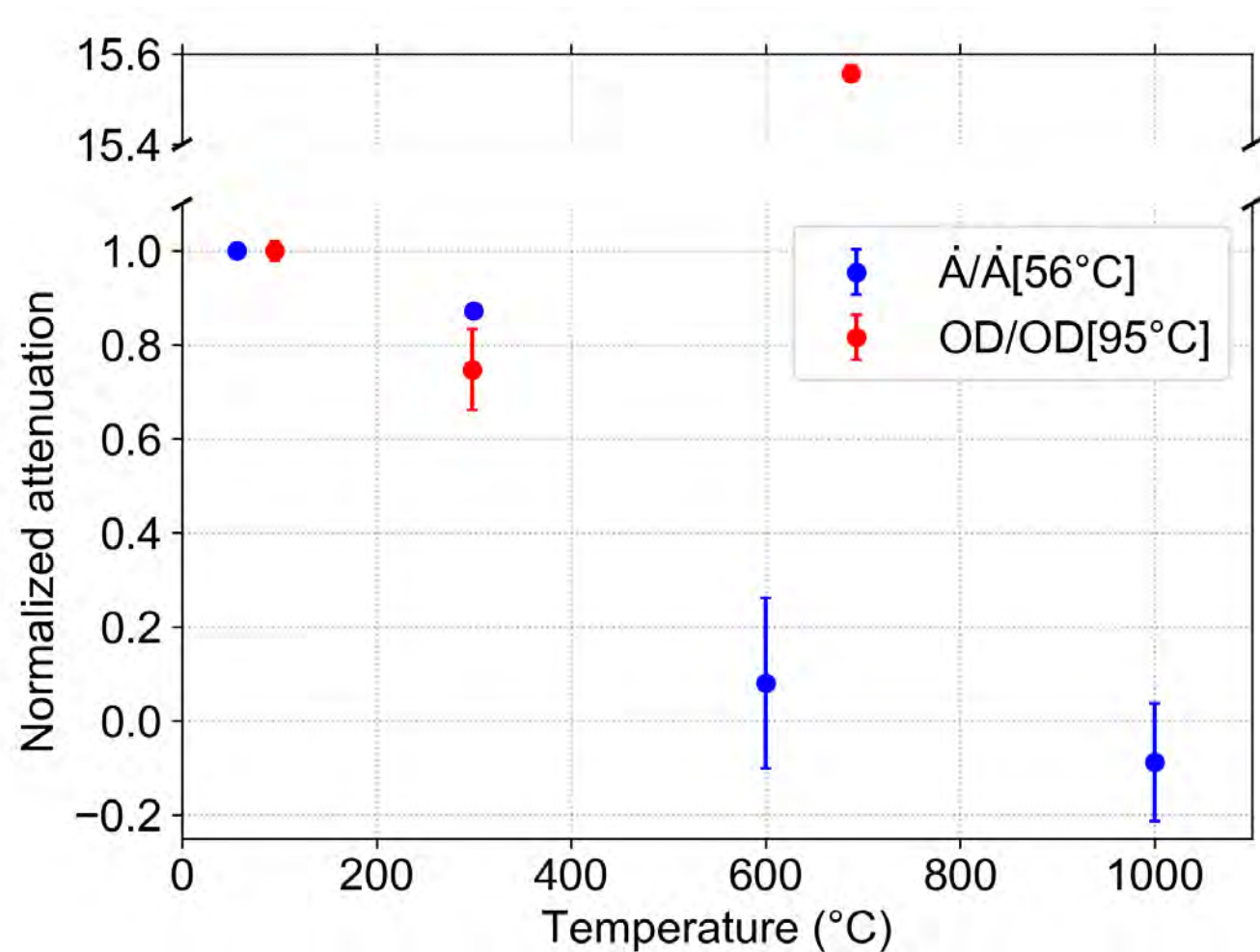


[1] C.M. Petrie et al., "Optical transmission and dimensional stability of single-crystal sapphire after high-dose neutron irradiation at various temperatures up to 688°C," *Journal of Nuclear Materials* 559 (2022) 153432.

[2] C.M. Petrie et al., "High-Dose Temperature-Dependent Neutron Irradiation Effects on the Optical Transmission and Dimensional Stability of Amorphous Fused Silica," *Journal of Non-Crystalline Solids* 525 (2019) 119668.

# Comparison to previous low neutron fluence in situ measurements

- High neutron fluence testing [1]
  - Post-irradiation attenuation (or optical density, OD) measurement
  - OD at 650 nm normalized to value measured after irradiation at 95°C
  - $1.1 \times 10^{15}$  n/cm<sup>2</sup>/s fast flux
  - $2.4 \times 10^{21}$  n/cm<sup>2</sup> fast fluence
- Previous low neutron fluence testing [2]
  - In situ measurement
  - Attenuation rates ( $\dot{A}$ ) at 650 nm normalized to value during irradiation at 56°C
  - $6.3 \times 10^{10}$  n/cm<sup>2</sup>/s fast flux
  - $6.9 \times 10^{15}$  n/cm<sup>2</sup> fast fluence
- Clearly very different temperature trends, suggesting different phenomena at low vs. high neutron fluence

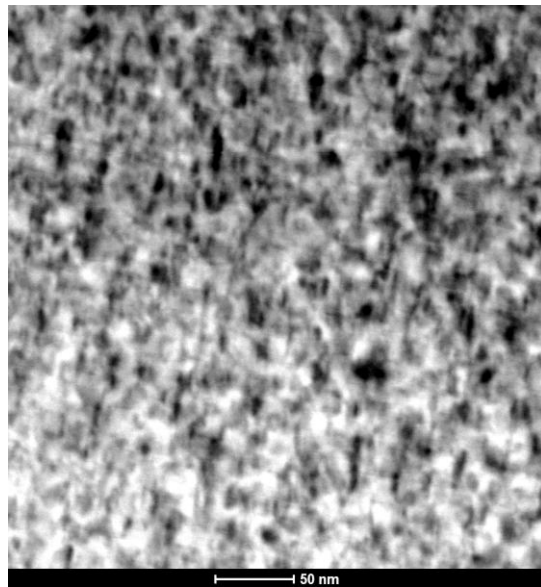


[1] C.M. Petrie et al., "Optical transmission and dimensional stability of single-crystal sapphire after high-dose neutron irradiation at various temperatures up to 688°C," *Journal of Nuclear Materials* 559 (2022) 153432.

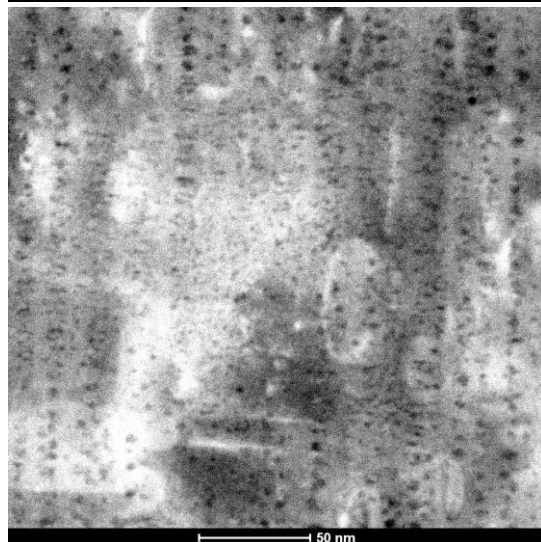
[2] C.M. Petrie and T.E. Blue, "In-situ reactor radiation-induced attenuation in sapphire optical fibers heated up to 1000°C," *Nuclear Instruments and Methods in Physics Research B: Beam Interactions with Materials and Atoms* 342 (2015) 91-97.

# Current theory: Rayleigh scattering losses from radiation-induced voids that occur at high dose and temperature

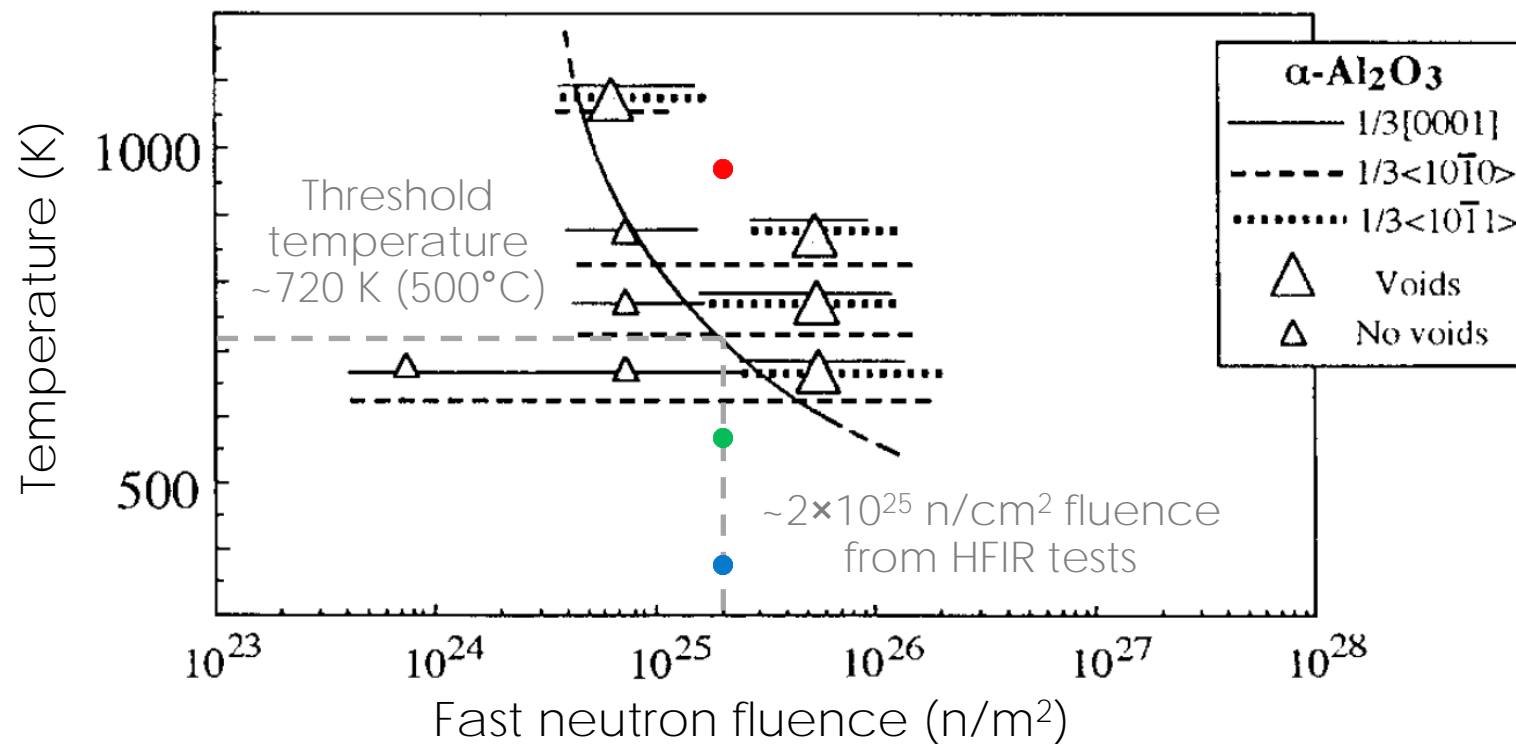
298°C:  
Dislocation  
loops, no  
voids



688°C:  
Voids  
aligned  
along c-  
axis



- Observations of voids oriented along c-axis consistent with previous literature
  - Requires temperatures  $>500^{\circ}\text{C}$  for fluence tested in HFIR
- Void diameter ( $\sim 3\text{ nm}$ )  $\ll \lambda$  ( $\sim 1\text{ }\mu\text{m}$ ),  $n_{\text{void}} \approx 1$
- Observed  $\lambda^{-4}$  attenuation dependence consistent with theory

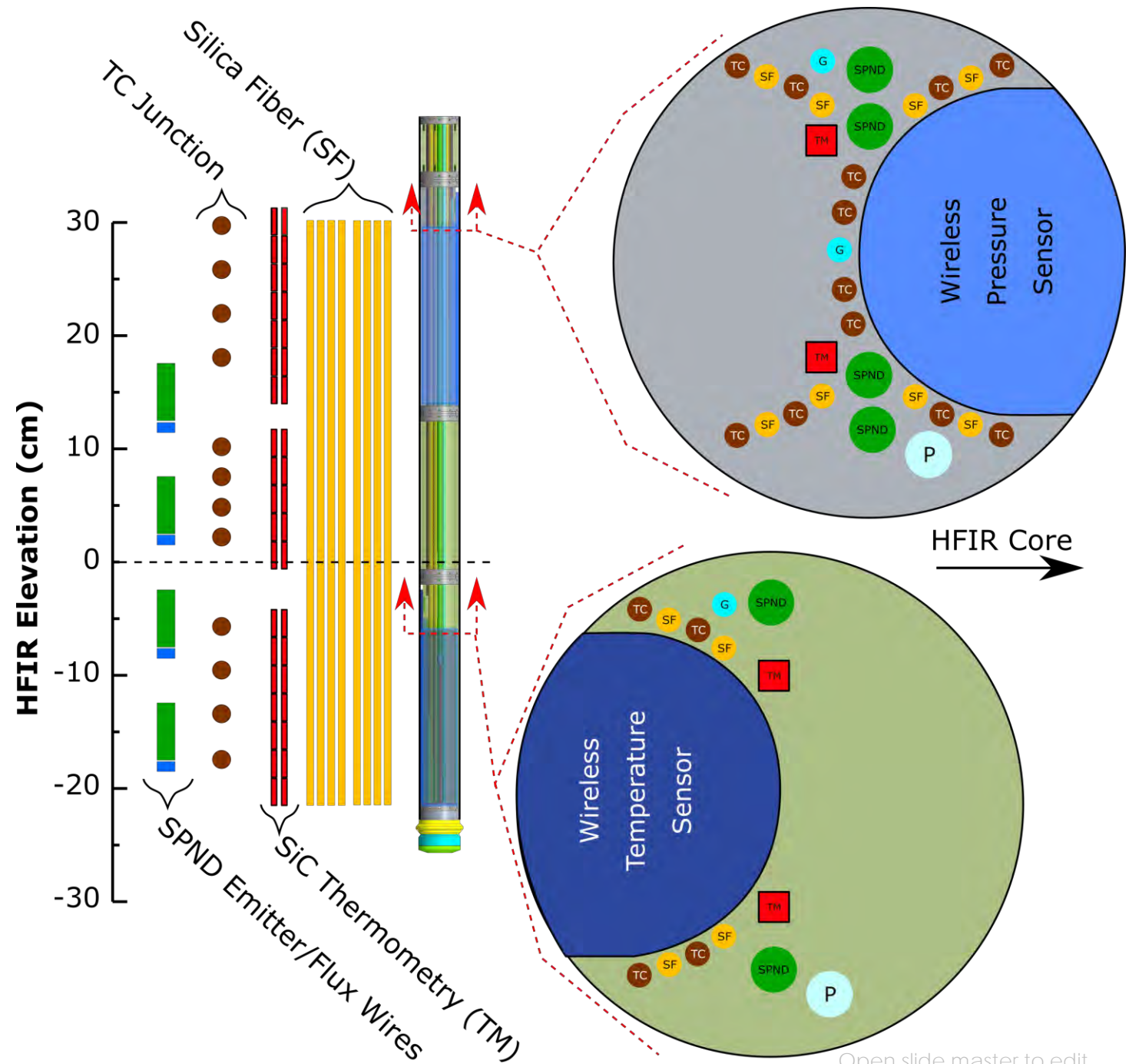


[1] C. Kinoshita and S.J. Zinkle, "Potential and limitations of ceramics in terms of structural and electrical integrity in fusion environments," *Journal of Nuclear Materials* 233–237 (1996) 100–110.



# WIRE-21 experiment

- Primary goal: Evaluate effects of high neutron fluence on WEC's wireless sensors in the High Flux Isotope Reactor (HFIR) at LWR temperatures ( $\sim 300^\circ\text{C}$ )
- Secondary goal: Characterize temperature and flux distributions with additional instrumentation
  - Thermocouples
  - Distributed fiber optic temperature sensors
  - Self-powered neutron detectors (V emitter)
  - Passive SiC TMs and flux wires
- Most highly instrumented experiment in HFIR's history
- High neutron flux:  $\sim 5 \times 10^{14} n_{\text{fast}}/\text{cm}^2/\text{s}$
- $\sim 50$  cm length within fueled region of the core



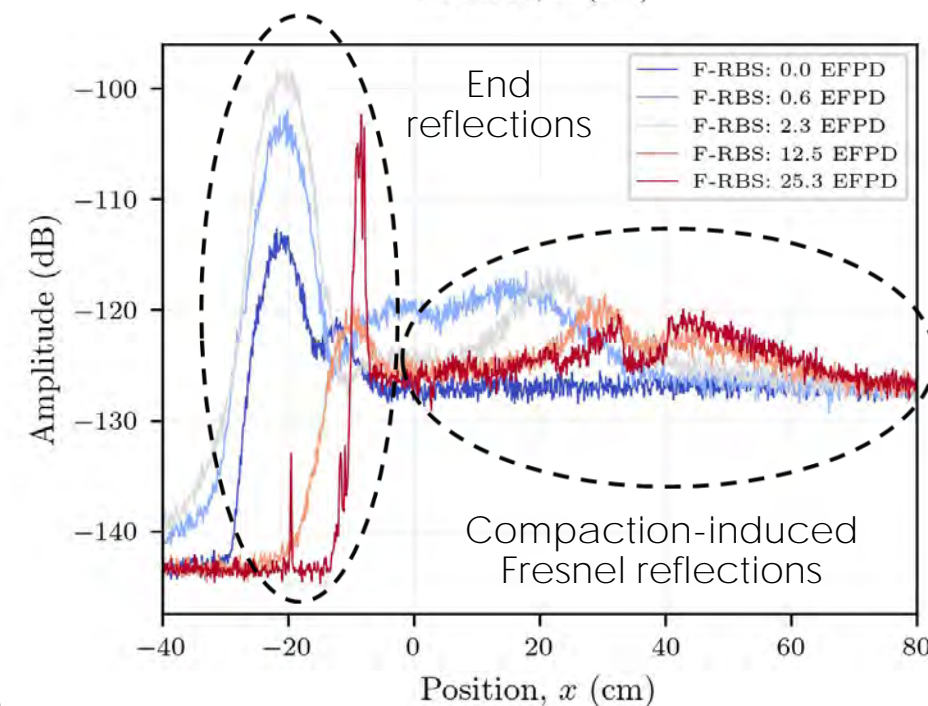
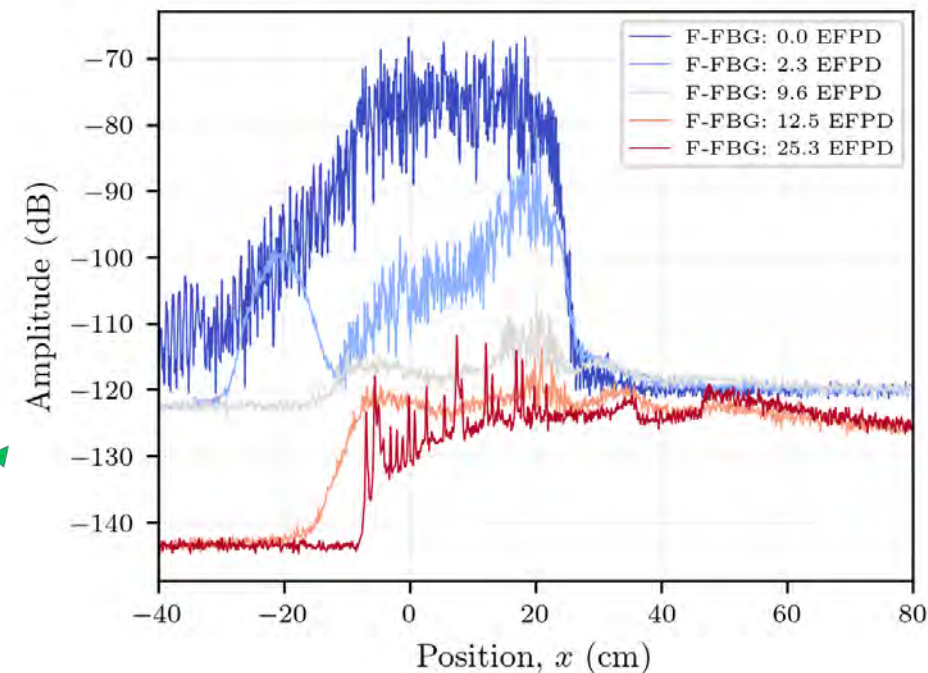
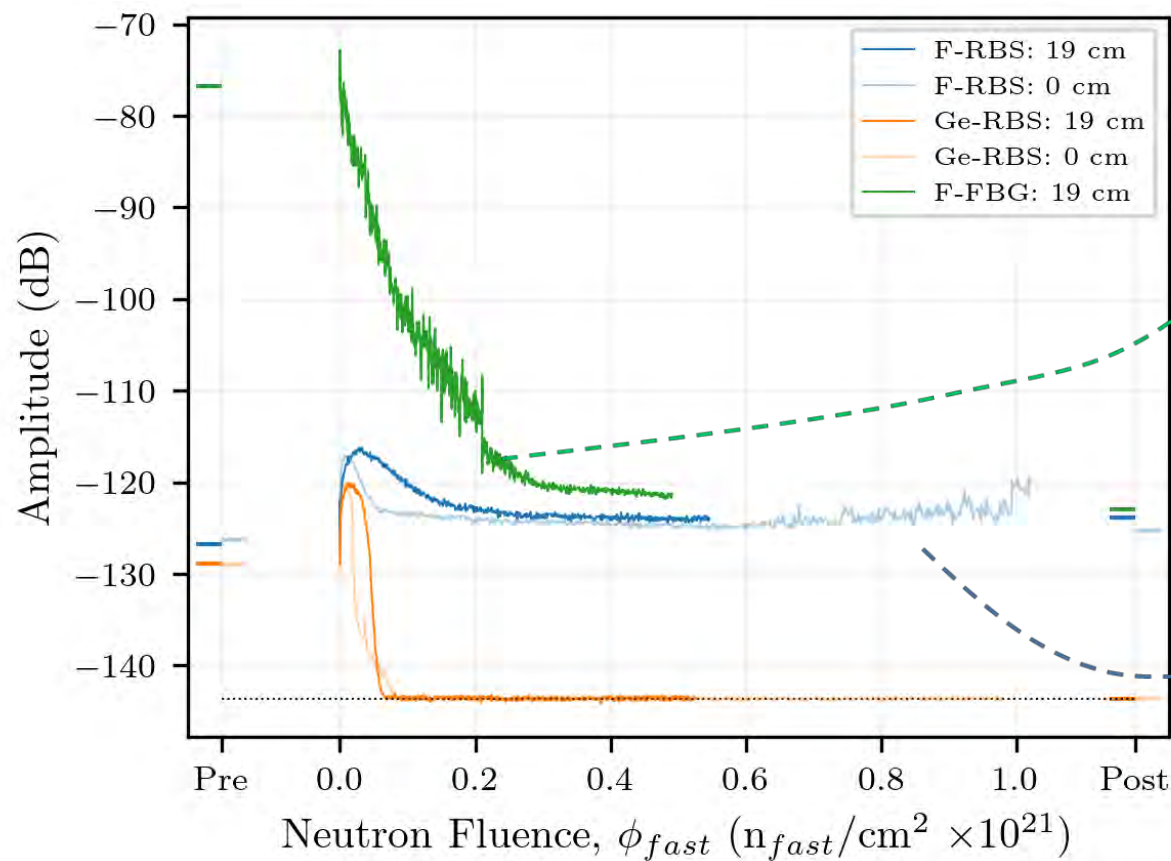
# In situ measurements of a-SiO<sub>2</sub> fiber sensors

- Primarily focused on radiation-hardened fibers
  - Pure SiO<sub>2</sub> core, F-doped SiO<sub>2</sub> cladding
  - Hollow core photonic crystal fibers
  - Ge-doped core fibers as a reference
- Fibers included with and without fiber Bragg gratings (FBGs)
  - Type I and Type II
- Optical backscatter reflectometry measurements made every 5 minutes
  - 1530–1572 nm
  - Allows measurement of spatial variations in reflected amplitude (attenuation) and local spectral shifts
  - Data processed using previously-established adaptive reference techniques to continuously resolve shifts relative to start of experiment

Fiber	Description	Gratings
1	Pure SiO <sub>2</sub> core, F-doped SiO <sub>2</sub> cladding	N/A
2	Ge-doped SiO <sub>2</sub> core, pure SiO <sub>2</sub> cladding	
3	F-doped SiO <sub>2</sub> core and cladding with 6–9 Type II gratings	~1% reflectivity, ~65 mm spacing
4		
5	Pure SiO <sub>2</sub> core, F-doped SiO <sub>2</sub> cladding with 28 Type II gratings	~3% reflectivity, ~10 mm spacing
6	Ge-doped SiO <sub>2</sub> core, pure SiO <sub>2</sub> cladding with ~120 Type I gratings	<0.1% reflectivity, 10.5 mm spacing
7	Hollow core photonic crystal fiber	N/A
8		

# Reflected amplitudes

- Ge-doped fiber amplitudes quickly reduced to noise floor
- F-doped fiber amplitudes reach equilibrium values *higher* than pre-irradiation values
- Amplitudes from Type II FBGs in F-doped fiber approach those of non-grated fiber

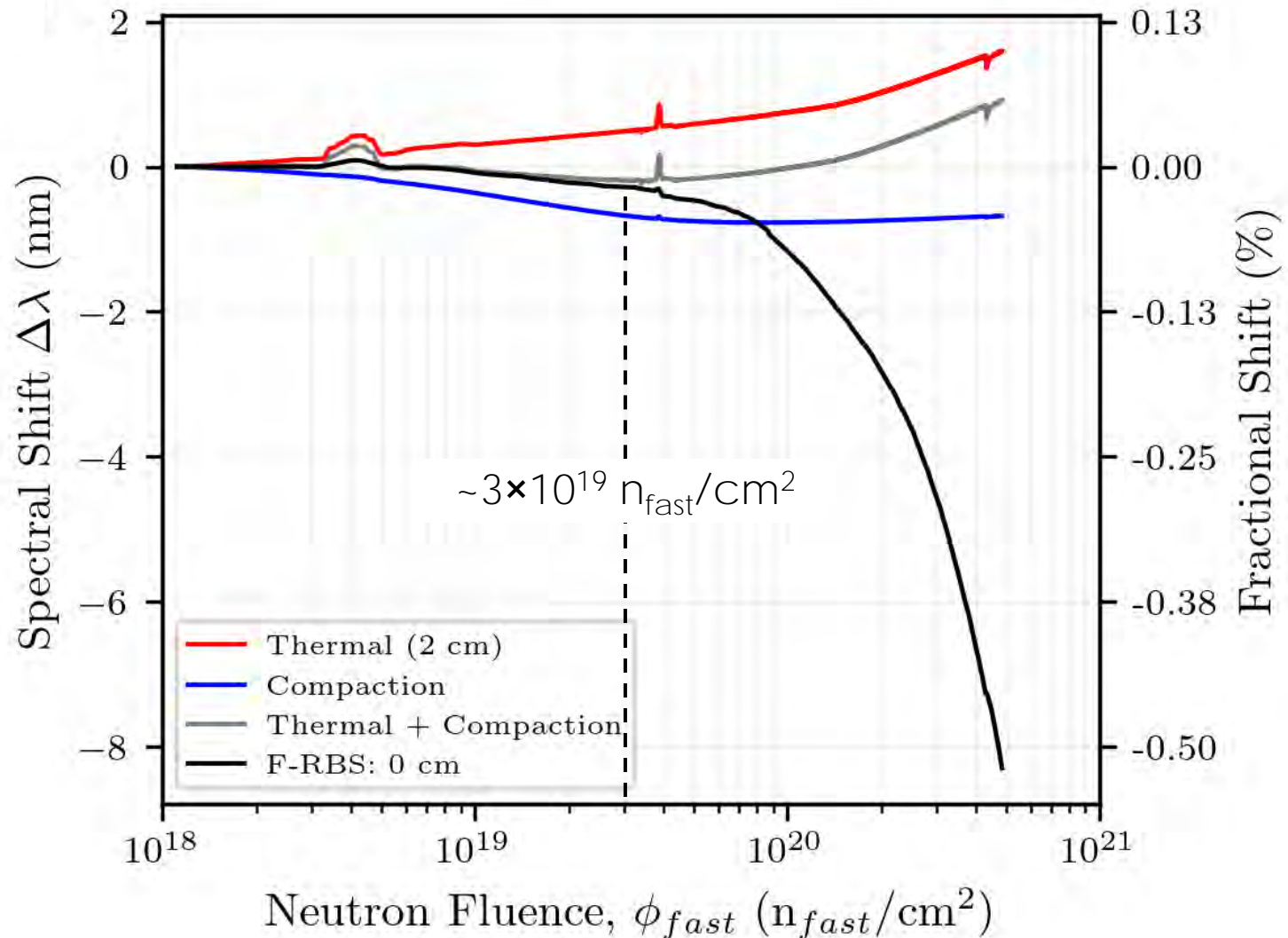


[1] C.M. Petrie and D.C. Sweeney, "Enhanced backscatter and unsaturated blue wavelength shifts in F-doped fused silica optical fibers exposed to extreme neutron radiation damage," *Optica* (under review).



# Spectral shifts

- Drift in a-SiO<sub>2</sub> fibers expected due to compaction
  - Predictive models developed previously [1]
  - Negative dL/L, positive dn/n, net blue shift (lower wavelengths)
  - Should reach equilibrium below 10<sup>20</sup> n<sub>fast</sub>/cm<sup>2</sup>
- Model accurately captures drift up to  $\sim 3 \times 10^{19}$  n<sub>fast</sub>/cm<sup>2</sup>
- Unsaturated drift begins at higher fluences
  - Cannot be explained by previous measurements of compaction and refractive index at even higher neutron fluence

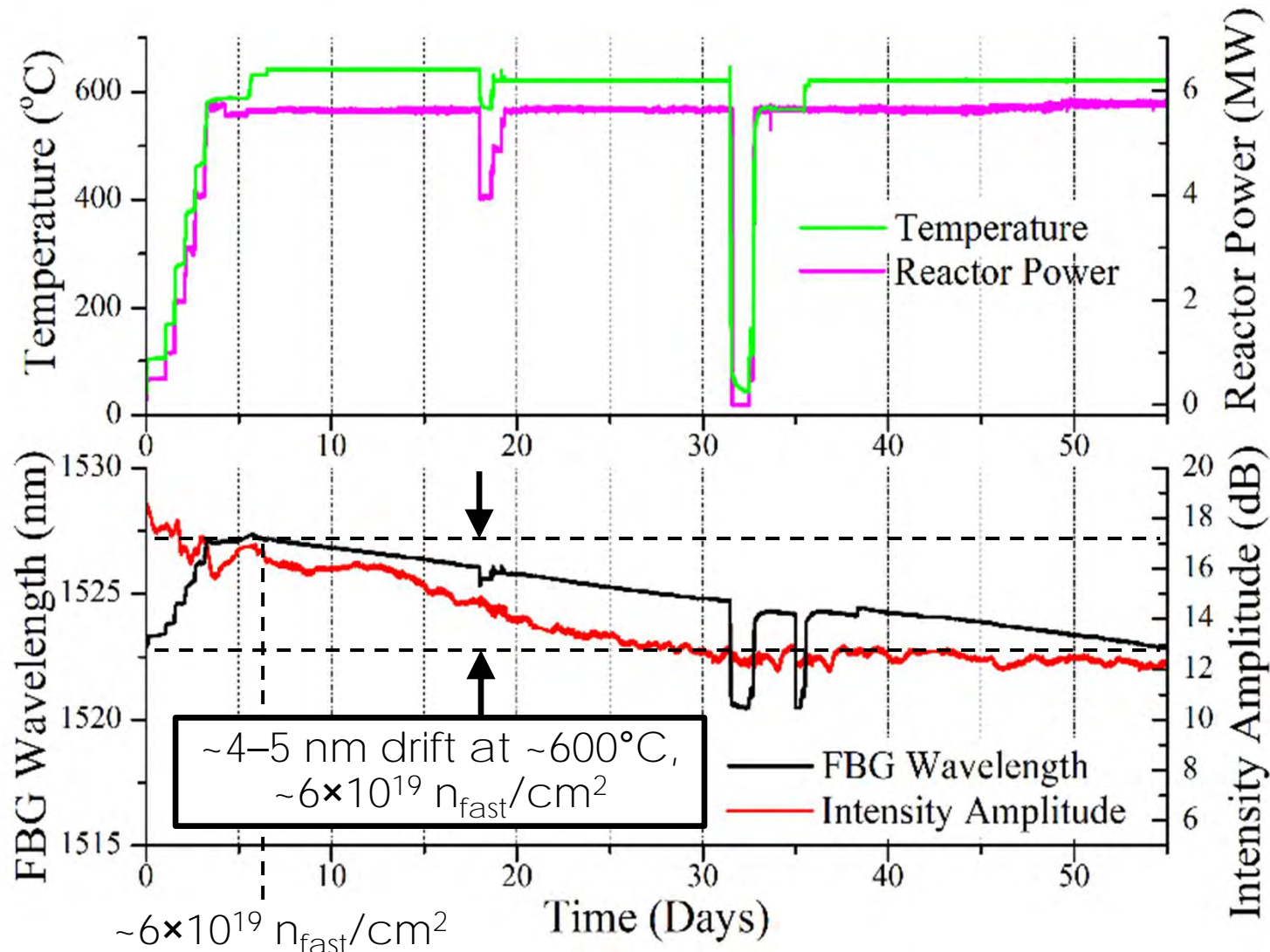


[1] C.M. Petrie et al., "High-Dose Temperature-Dependent Neutron Irradiation Effects on the Optical Transmission and Dimensional Stability of Amorphous Fused Silica," *Journal of Non-Crystalline Solids* 525 (2019) 119668.

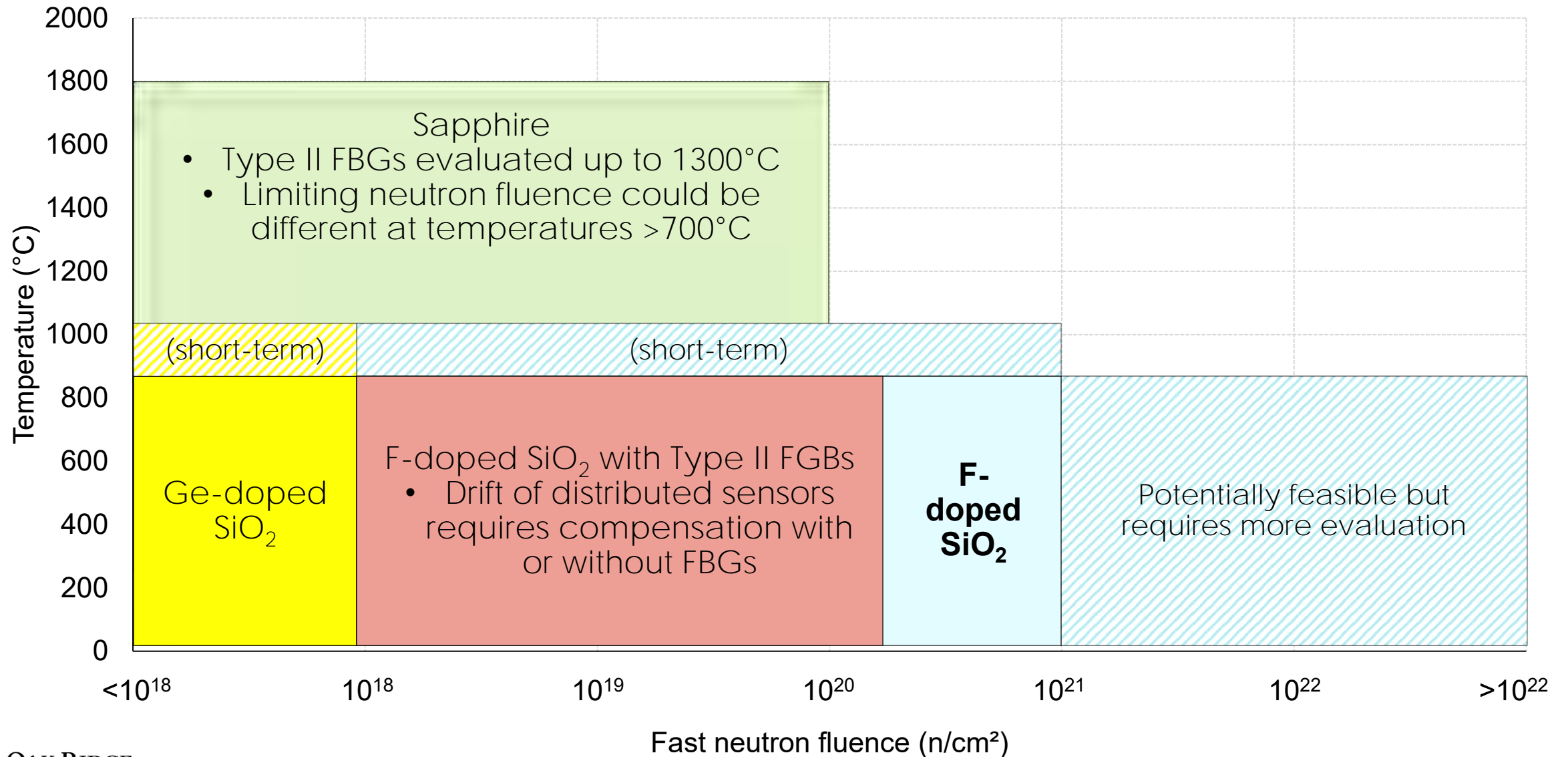
[2] C.M. Petrie and D.C. Sweeney, "Enhanced backscatter and unsaturated blue wavelength shifts in F-doped fused silica optical fibers exposed to extreme neutron radiation damage," *Optica* (under review).

# Similar linear drift observed previously in FBGs in random air-line fibers

- Consistent trends observed in fibers irradiated with/without FBGs in both F-doped SiO<sub>2</sub> fibers and SiO<sub>2</sub> fibers with random air-lines
- Fluence at which unsaturated drift begins could depend on temperature, dose rate, fiber type, FBG type, etc.



# Windows of operation







Questions?  
Chris Petrie, [petriecm@ornl.gov](mailto:petriecm@ornl.gov)